Wall turbulence and turbulent drag reduction

Paolo Luchini[1][0000−0001−6527−7762] and Maurizio Quadrio[2][0000−0002−7662−3576]

[1] Università di Salerno, DIIN, Fisciano, Italy
[2] Politecnico di Milano, DAER, Milano, Italy

Abstract. Fluid flow turbulence is probably the last unsolved mystery of classical physics. Research groups are active all over the World with the double aim to accumulate ever more precise empirical knowledge (using a synergy of experiments and numerical simulations), and to frame this empirical knowledge into a consistent theory that may prove of predictive value for applications. Italian Mechanics strongly participates in this effort. Here progress is described in the comprehension of wall-bounded turbulence and the reduction of turbulent skin-friction drag, in their four aspects of the shape of the mean velocity profile, the statistics of turbulent fluctuations, devices of passive drag reduction and devices of active drag reduction. An inevitable bias will be seen for the topics to which the present authors have contributed directly, but these are also the results that we can more easily entice the reader with.

Keywords: Fluid mechanics · Turbulence · Drag reduction.

1 Introduction

To sketch a history of our understanding of turbulence and turbulent flow, at any level of detail, is a daunting task. In this chapter we take up the limited goal of sketching part of the Italian contributions to the subject, with a focus on our own contributions. Discussion is limited to the specific type of turbulence that takes place in the vicinity of a solid wall. Since the most practically relevant manifestation of the onset of turbulence in wall-bounded flow is its increased skin-friction drag, developments in studies, concepts and technologies for turbulent skin-friction reduction will also be given particular emphasis.

The notion that turbulence near a wall possesses a certain degree of structure emerged half a century ago, and is slowly superseding the concept (still embedded in some current RANS turbulence models) that a turbulent flow is just random and unpredictable overall, and approaches the laminar state once the very near-wall layer is reached. Lexically, this corresponds to the terminology shift where this layer, once called laminar sublayer, is now referred to as the viscous sublayer.

Around the middle of the past century, early flow visualizations provided the first evidence of the streaky structure of the flow in the near-wall region. The qualitative nature of such early visualizations notwithstanding, they exposed the organized character of the flow, and immediately raised the question of the dynamical significance of such organized motions. Attempts to create a link between visualizations and Reynolds stresses quickly led to the notion of near-wall

"events" (the dominant ones being called ejections and sweeps). Their contribution was typically categorized via the quadrant analysis, which is still in use, and quantifies the contribution of different events to the Reynolds shear stresses starting from a time history of a pointwise measurement of the longitudinal and wall-normal velocity components, typically performed with a two-component hot-wire probe. This is where the first conceptual models of turbulence started to appear. Conditional sampling and, more importantly, conditional averaging techniques (the latter implying the ability to store a large measurement dataset and process it later on, something that became available at the same time as computers gradually evolved in power) marked one further step in the characterization of wall turbulence, leading to additional means to characterize the importance of near-wall coherent structures.

The last step connecting the pioneering era to modern times is the advent of direct numerical simulation (DNS) of wall turbulence. It's generally marked to begin with the publication of results from the first DNS of a turbulent channel flow, by Kim Moin & Moser in 1987 [28], following nearly a decade of preparation and development of the numerical approach that predated the actual availability of the necessary computing power. DNS revolutionized our way of looking at wall turbulence, since its limitations are largely complementary to those of the experimental approach, and opened up novel ways of studying its physics.

2 The structure of the mean velocity profile

The mean velocity profile is definitely the most important quantity of interest. Nearly a century ago, Prandtl recognized by his mixing-length argument that the mean turbulent velocity profile in a pipe or channel would have to be approximately logarithmic in shape. The theory was then refined by von Kármán, and given its present-day form based on dimensional analysis by Millikan. Their argument applies, in a suitable range of distance from the wall, to basically all wall-bounded turbulent flows.

The essence of the Prandtl–von Kármán–Millikan theory sits in scale separation between a "viscous" layer where the wall-normal coordinate z is of the order of the viscous length[3] $\ell \equiv \nu/u_\tau$, and a "defect" layer where z is of the order of the macroscopic scale h of the flow (say, the half-distance between parallel walls or the radius of a pipe, or the thickness of a boundary layer). The ratio h/ℓ coincides with the shear-based Reynolds number $\mathrm{Re}_\tau \equiv u_\tau h/\nu$, and thus scale separation arises naturally in the turbulent asymptotic limit of $\mathrm{Re}_\tau \to \infty$. Dimensional analysis dictates the functional form of the velocity profile in either layer, and the ansatz that the velocity function be independent of both ℓ and h where the two layers overlap, for $\ell \ll z \ll h$, leads to the conclusion that in this region the functional form of the velocity profile $u(z)$ must be logarithmic with

[3] with ν denoting kinematic viscosity, and $u_\tau \equiv \sqrt{\tau_{\mathrm{wall}}/\rho}$ the characteristic velocity of turbulent fluctuations, based on the wall shear stress τ_{wall} and fluid density ρ.

universal coefficients κ (named von Kármán's constant) and B:

$$\frac{u}{u_\tau} \equiv u^+ = \frac{1}{\kappa}\log(z^+) + B, \quad \text{with} \quad z^+ \equiv \frac{u_\tau z}{\nu}. \tag{1}$$

This century-old formula is one of the mainstays of turbulence theory and is taught in all basic textbooks about it, yet it has been the target of continued debate, with a large fraction of scientists contending the universality of constant B, a smaller crowd contending the universality of κ, and a few loudly proposing outright alternative formulas which are not logarithmic. In fact the fit of (1) to both experimental and numerical-simulation data exhibits measurable deviations with geometry, and a worldwide effort is ongoing to explain such deviations and to measure von Kármán's constant, a measurement made difficult by the very presence of deviations even for those scientists who believe κ (and/or B) is indeed a universal constant of Nature. Short of denying (1) altogether, one must evince that deviations from (1) only disappear at values of the Reynolds number that are beyond those achieved by up-to-present experiments and numerical simulations. Trust in (1) would be much higher, and a precise measurement of von Kármán's constant from present data would become feasible, if the observed deviations could be explicitly accounted for in the form of higher-order corrections to the asymptotic theory underpinning the logarithmic law. Research has thus focused on one hand upon enlarging the Reynolds-number range that experiments and numerical simulations can afford, on the other upon higher-order asymptotic theories able to explain the present data at present values of Re.

An important effort towards increasing the Reynolds-number range of velocity-profile measurements is the CICLoPE project. Based near Predappio (Italy) inside a long tunnel escavated during war times by the aeronautical Caproni industries, and managed by the University of Bologna under the supervision of A. Talamelli and G. Bellani, CICLoPE (Centre for International Cooperation in Long Pipe Experiments) is an international cooperation that built a 115m-long circular pipe of 0.9m$\pm$0.1mm diameter where air can flow at up to 60 m/s. The facility was inaugurated in 2015 and has been hosting a large number of projects since. Details can be found at `https://www.euhit.org/infras/ciclope/`.

A simple higher-order extension of the logarithmic law that allows a single set of κ and B constants to fit velocity profiles in different geometries starting at $\mathrm{Re}_\tau \gtrsim 400$ was proposed by one of the present authors [36]. Already noticed by Afzal [1] and Jimenez and Moser [25] had been that if the pressure gradient p_x is assumed as a perturbation parameter in an asymptotic theory of the velocity profile, a dimensional argument leads the dimensionless pressure gradient to contain the first power of the wall-normal coordinate z; in other words, it leads to a velocity correction that is a linear function of z. Neither author, however, actually determined a value for the coefficient of this linear function or pushed the argument to its practical consequences for the experimental and numerical validation of the logarithmic law. From an overview of experimental and numerical data of a wide range of sources, Luchini [36,32] determined that the best fitting value of its coefficient (named A_1) is near unity, leading to the conjecture

that it may actually be $A_1 = 1$, and thus to the higher-order logarithmic law

$$u^+ = \frac{1}{\kappa}\log(z^+) + B - \frac{p_x}{\tau_{\text{wall}}}z. \tag{2}$$

Equation (2) fits the velocity profile in all tested geometries (Couette and Poiseuille plane flow, Poiseuille circular pipe flow, boundary layer) with common values

$$\kappa = 0.392, \quad B = 4.48 \tag{3}$$

of the classical coefficients (most notably with a single value of the B coefficient, which most previous analyses, even those assuming that κ is universal, concluded to change with geometry [40]). Von Kármán's constant κ thus comes out in agreement with a specific one of the previous proposals, the value of 0.39 extracted by the Australian school [42] from experimental measurements of the friction law in place of the velocity profile, and in contrast to historical estimates of $0.40 \div 0.41$. In addition, interpolating formulas for the wall layer and the defect layer were also provided (see Box 1 and Eqs. 27, 29, 30 of [32]), arriving at a uniform formulation that describes the velocity profile over the entire range of $0 \le z \le h$ and all geometries (Eq. 1 and Fig. 2 of [38]). Particularly satisfying was the comparison of the present theory with the independently performed Hi-Reff pipe-flow experiment [19], reproduced as Fig. 1 here. An application range was also determined, that this formulation works well within available experimental accuracy for all $\mathrm{Re}_\tau \gtrsim 400$, and that the logarithmic portion of it prevails in the range $200\ell \lesssim z \lesssim 0.5h$ (whereas competing theories [44] surmise that an asymptotic regime is only attained for Re_τ greater than approximately 30000).

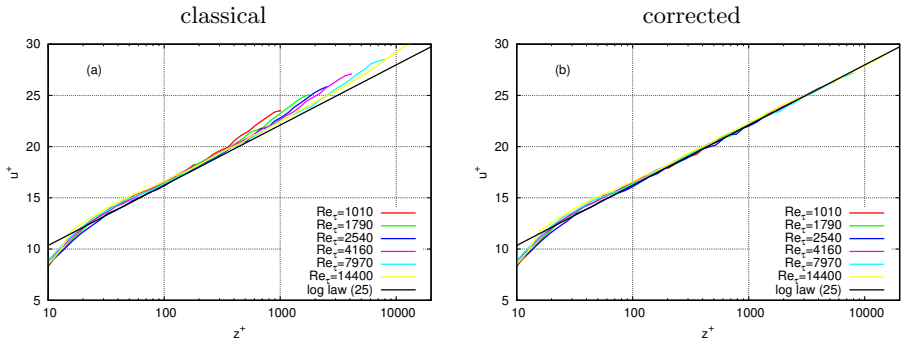

Fig. 1. Fit of the classical logarithmic law (1) and of the corrected logarithmic law (2) to the Hi-Reff pipe-flow experiments. From [38]

Further developments ensued in yet more recent times. Once taken for granted that deviations from the turbulent logarithmic law are to be ascribed to the pressure gradient, one can quantitatively compare them to analogous deviations

(from the rectilinear, zero-pressure-gradient Couette profile) that take place in laminar flow. Luchini [37] highlighted that this deviation is of opposite sign in laminar and in turbulent flow. That is, if in laminar flow the presence of a favourable, negative pressure gradient decreases the flow rate for a given wall shear stress (or equivalently, increases the wall shear stress for a given flow rate), in turbulent flow it increases the flow rate for a given wall shear stress (decreases the wall shear stress for a given flow rate). Astounding as this behaviour is, it is actually consistent with (one could say, it explains) some previous equally astounding observations: in particular, the conclusion by Johnstone *et al.* [26] that a mixing-length turbulence model based on the wall shear stress offers a better adherence to reality than a mixing-length model based on the local shear stress (whereas considerations based on the locality of eddy viscosity would favour the latter, and those authors were actually surprised at their own result); and the conclusion by Russo and Luchini [54] that the response of channel flow to a vertically varying volume force with zero mean (meant, in that context, to mimic the action of a wavy bottom) is of opposite sign in laminar and in turbulent flow. These observations have far-reaching implications for the future of turbulence modelling, because most current turbulence models based on eddy viscosity are bound to predict a same-sign behaviour of laminar and turbulent flow in all of these configurations.

3 Statistical characterization of wall turbulence

Besides the mean velocity profile there are other statistical quantities of interest in wall turbulence, most prominently the second-order moments of velocity fluctuations; these relate to turbulent energy, a quantity of practical interest. The experiments we already mentioned endeavoured to measure these quantities at the same time as the mean velocity profile. So did direct numerical simulations; the canonical wall-bounded flows (the plane channel, either pressure or shear-driven, and the cylindrical pipe) were considered early in DNS history, and several Italian groups took part in the international effort at progressively increasing the computational scale of the simulations and the achievable Reynolds number. Among several important contributions, one may recall the many ones by P. Orlandi and coworkers [9], the recent, record-setting pipe flow DNS at $\mathrm{Re}_\tau = 6000$ by Pirozzoli *et al.* [46], and the open-source codes made available to the research community for massively parallel and GPU-based computations, for both incompressible [58] and compressible [10] flow.

The present authors, while contributing their own DNS code and approach [34] which is however not aimed towards high-Re simulations, have focused their efforts upon less conventional descriptions of the same class of flows. For example they were among the first to consider the full space-time structure of the turbulence statistics [50], thus separating the physical correlation from the spurious effects of the computational periodic box. They also pioneered the (admittedly simple) idea of considering DNS output (say, the mean velocity at a particular wall distance) as affected by measurement error, as any experimentalist would

be naturally inclined to do, and to propose to augment DNS results with an error bar representative of the uncertainty related to the statistical-averaging process. In the presence of homogeneous directions, one typically uses statistical averages over finite time and space windows to arrive at estimates of the true expected value, and a rational criterion to properly select such windows is necessary. Albeit at different levels of complexity, this concept [21,45,54,55] is progressively becoming accepted by the community.

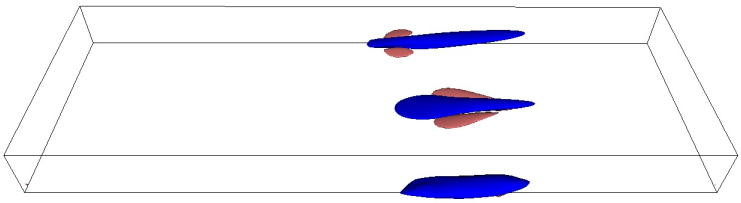

Fig. 2. Streamwise component of the longitudinal-velocity response to a wall-normal velocity impulse. The figure plots, at a time separation of $\tau^+ = 30$ after the impulse, isosurfaces of the positive (red) and negative (blue) response in the three cases of laminar flow (top), laminar flow linearized about the mean turbulent profile (center) and full averaged turbulent response (bottom). Taken from [49].

An original statistical quantity was proposed by the authors [49] in order to describe a turbulent channel flow in terms of its complete mean impulse response to a perturbation applied at the wall. This tensorial quantity (that can in principle also be measured experimentally) is a symmetric second-order tensor where the independent variables are the time delay and the 3 spatial coordinates expressing separation from the point at the wall where perturbation is applied. It can be easily defined in the laminar case, while in the turbulent case this quantity is important whenever one attempts to control the flow by using linear control theory, for which the mean response constitutes the best model of the dynamical system. The very definition of the impulse response for a turbulent flow involves two non-trivial conceptual steps: first the mean response must be defined, as the instantaneous one is unavoidably bound to diverge; and then the response must be actually measured, by circumventing the practical difficulty that linearity of the response requires small forcing perturbations at the wall, which may easily be overwhelmed by the comparatively large noise of turbulent fluctuations. An ingenious measurement strategy was devised [35], exploiting the fact that passing a white noise through a linear system and measuring the correlation between its input and output yields the impulse response of the system. Figure 2 displays the difference between the correct response, accounting for turbulent diffusion, and the one obtained by simply using linearized equations about the mean turbulent

velocity profile. A similar impulse-response concept, extended to measure the response to a volume forcing, was later used in the already mentioned work [54].

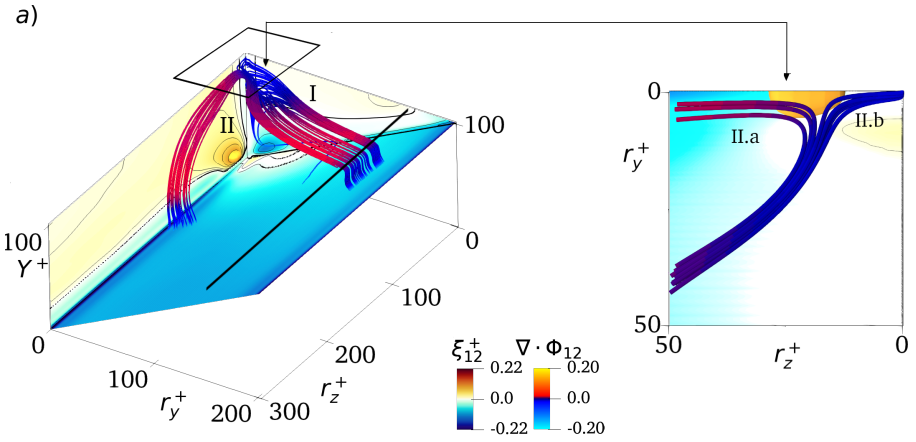

Fig. 3. Spatial and scale fluxes of the structure function $\langle \delta u \delta v \rangle$ in a turbulent Couette flow at $Re_\tau = 100$. Flux lines are drawn together with a colormap (on the bounding planes) of the source term, in a three-dimensional space where the coordinates are the wall-normal distance Y^+ and the spanwise and wall-normal separations r_z^+ and r_y^+. Taken from [12].

A further innovation to be mentioned here is a general description of the second-order moments of velocity fluctuations, which naturally links together the concept of energy cascade in the space of scales, along the lines of the Richardson–Kolmogorov theory, and the concept of Reynolds stresses varying with the distance from the wall, yielding fluxes in physical space. In fact, the single-point budgets for the Reynolds stresses [39] lack information about the scales involved in their fluxes, and miss the multi-scale nature of turbulence, whereas a spectral decomposition does discern different scales, but fails to provide direct information on their role in production, transfer and dissipation of turbulent kinetic energy. About 20 years ago, Hill [24] generalized the classic Kolmogorov equation for the second-order structure function (or, equivalently, the Kármán–Howart equation for the correlation tensor) from homogeneous and isotropic turbulence to inhomogeneous turbulent flows. The generalized Kolmogorov equation was the tool of choice for studying the scale energy in several flows, ranging from simple wall-bounded flows to shear layers; Italian contributions [13,15,14] are prominent in this thread. Most recently, Gatti *et al.*[20] further extended the concept to deal with anisotropy. They derived exact budget equations for the second-order structure function *tensor*: the anisotropic generalised Kolmogorov equations (AGKE) describe the production, transport, redistribution and dissipation of each Reynolds stress component occurring simultaneously among different scales and in space, i.e. along directions of sta-

tistical inhomogeneity. AGKE provide a natural definition of scales in inhomogeneous directions, and describe fluxes across such scales too. AGKE are being used to describe the structure of turbulence, in the compound space of scales and positions, starting from the simple turbulent Poiseuille flow, to the same flow at higher Re, where it is found that AGKE quantities start very soon to highlight the structure of the outer turbulent cycle. Couette flow has been investigated too [12], producing an explanation of the complex direct/inverse and ascending/descending cascade taking place in a turbulent Couette flow, where the near-wall cycle coexists with large streamwise vortices which fill the entire gap between the walls. A sample result is shown in figure 3, where fluxes of the off-diagonal component $\langle \delta u \delta v \rangle$ in the subspace (r_z^+, r_y^+, Y^+) are drawn together with the source term that denotes net production of shear stress.

4 Passive drag reduction and riblets

The reduction of turbulent drag in wall-bounded flow is an obvious technological goal. The most practical means of turbulent-drag reduction is passive, consisting of static modifications of the solid wall surface or of the fluid's composition, as opposed to active (discussed in next section), which involves moving parts and energy expenditure.

Most effective among the methods of passive drag reduction is the injection of tiny amounts of soluble long-chain polymers, which can provide up to 80% skin-friction reduction [57] by a non-Newtonian mechanism which still today cannot be said to be totally understood. Examples of Italian research contributions on this topic are [8,17,16]. The drawbacks of this method are, of course, that it can only be used in liquids and that polymers are consumed continuously and dispersed into the working fluid. It has found important applications in oil pipelines, although these will not be reviewed here.

Wall-surface modifications provide a more modest advantage, of the order of 10% reduction at best, but can be applied in any fluid, and are the most promising drag-reduction devices for aeronautical, marine or terrestrial vehicle applications. The present authors, in particular, have contributed to clarifying the operating mechanism of the so called "riblets", long and fine ridges (or grooves, if seen on the negative side) directed parallel to the flow on the wall surface. It appears at first sight counterintuitive that such a non-smooth surface may have a lower drag than a perfectly smooth one, but similar surfaces exist in nature: the empirical idea that riblets could reduce drag came about early, after the observation that similar structures are present on the scales of shark skin (M.O. Kramer patented it in 1939). Only later, proceeding from the observation that the drag-reducing action of riblets occurs in a size range (≈ 15 spanwise in units of the length ℓ defined near (1), also known as "wall units") which is relatively small compared to the near-wall structures of turbulence (≈ 100 wall units), Bechert and Bartenwerfer [6] and Luchini *et al.* [33] proposed that their action could be explained through a virtual displacement of the wall represented by the viscous "protrusion height".

In the viscous layer that extends for the first few wall units above the surface, the physics of a turbulent flow is dominated by viscous forces (both in its mean value and in its fluctuations). Therefore the Navier–Stokes equations can be simplified in this region to the linear Stokes equations and, owing to linearity, longitudinal and transverse components can be studied separately and assigned, each, a separate protrusion height, this being the intercept with $u = 0$ of the straight line that the Stokes velocity profile tends to as $z \to \infty$. (For a general surface shape the protrusion height, also known as slip length, becomes a 2×2 symmetric tensor and the longitudinal and transverse protrusion heights are its principal values; see e.g. [31].)

Because of their simple definition based on Stokes flow, the longitudinal and transverse protrusion heights are unique for a given geometry, and scale linearly with spatial dimensions. In other words, the protrusion heights are geometrical parameters. Several examples of their values were provided in [33]. The protrusion heights are often measured from the riblet tips, but this is just a convention; the origin of the reference frame is arbitrary, and eventually only the difference of the two protrusion heights affects the flow. As an empirical computational observation this difference turns out to be very sensitive to sharpness of the tips, increasing with it; in fact, sufficient sharpness is not always easy to achieve in reality, and experiments conducted with razor blades [7] have shown that indeed the obtainable drag reduction is very sensitive to sharpness.

The physical explanation of the drag-reducing effect of riblets emerges from the observation that the differential action of riblets upon the longitudinal mean flow and the, prevalently transverse, turbulent eddies effectively pushes the eddies away from the wall and thus diminishes the near-wall turbulence level. This explanation was made quantitative by introducing the following ansatz [29,30]: *the law of the wall describing the mean-flow profile of the turbulent stream is modified by the presence of riblets only through a displacement of its origin by an amount equal to the difference of the two protrusion heights.* This ansatz derives its rationale from the idea that the turbulent fluctuations, and thus the Reynolds stresses, above riblets are the same that would persist if a plane wall was present at the position of the *transverse* protrusion height, whereas the mean flow (integral of the Reynolds stress) has its integration constant determined so that it vanishes at the *longitudinal* protrusion height.

Since in wall units the viscous tract of the velocity profile is $u^+ = z^+$, with a coefficient that becomes unity in this particular nondimensionalization, a displacement of the entire profile by an amount $\Delta z^+ = \Delta h^+$, where Δh^+ is the protrusion-height difference expressed in wall units, entails a velocity increase $\Delta u^+ = \Delta z^+ = \Delta h^+$. The displacement being rigid, this velocity increase remains constant for all z, and once attained the region where (1) prevails, it amounts to an increase of the B constant by $\Delta B = \Delta h^+$.

The classical theory of turbulent skin friction (and just as well its most recent variations: see e.g. §6 of [32]) dictates the following formula for the skin-friction coefficient c_f:

$$(c_f/2)^{-1/2} = \kappa^{-1} \log \left[(c_f/2)^{-1/2} \mathrm{Re}/2 \right] + B + C - D \tag{4}$$

where κ and B are the constants that appear in the logarithmic law of the wall (1), and C and D are characteristic constants of the outer layer unaffected by the wall's texture. From an expansion of (4) for small ΔB there follows equation (4) of [30]:

$$-\frac{\Delta c_f}{c_f} = \frac{\Delta B}{(2c_f)^{-1/2} + (2\kappa)^{-1}} = \frac{\Delta h^+}{(2c_f)^{-1/2} + (2\kappa)^{-1}}, \tag{5}$$

which provides a general quantitative expression of the relative skin-friction reduction as a function of the protrusion-height difference in wall units Δh^+. Equation (5) was verified by comparing it to an extensive number of test results [5] and found to agree reasonably well with the initial slope of the experimental drag curve if account is taken of the actual curvature radius of the riblet tips used in the experiments.

With increasing riblet size (usually measured by their spanwise repetition period s^+), the assumption that the action of riblets stay bounded to the viscous sublayer begins to fail. Drag reduction then ceases to be proportional to Δh^+. Eventually drag reduction saturates, and drag starts to increase again when the period s^+ grows beyond a threshold which empirically is $s^+ \approx 15$ [7]. The curve is not far from being parabolic, with a maximum drag reduction $1/2$ of the value given by (5) at $s^+ = 15$. What happens, in fact, is that the riblets' action no longer takes place in the portion of the velocity profile where $u^+ = z^+$, and therefore ΔB no longer equals Δh^+. Nevertheless the first half of (5) remains valid in a much larger range of sizes, as large as a logarithmic region exists, which is the case for the great majority of drag-reducing and drag-increasing devices. Even the classical drag increase produced by random sand roughness is nothing else than a negative ΔB, and the next Section will show how ΔB is a suitable parameter to describe the drag-reducing performance of active control as well.

5 Active techniques of drag reduction

In comparison to passive control, active control for skin-friction drag reduction carries the obvious drawbacks of extra complexity and extra energy expenditure. However, especially for relatively simple open-loop strategies, these drawbacks may be compensated by the larger savings. One family of active and open-loop techniques, referred to as spanwise forcing as it forces the boundary layer by injection of spanwise momentum in the near-wall region, has seen a major part of its development propelled by the Italian community [47].

With active control, the non-zero energy costs need to be accurately weighed against energy benefits before declaring a strategy effective. It is not uncommon to see massive "drag reduction" figures reported in the literature, with flow control strategies that cost way more than they save! The increasing importance of active control led to the formalization of the flow-control problem for skin-friction drag reduction [18,23], where a theoretical framework is developed for assessing drag reduction performance while properly accounting for the energy

cost of the control. It is now clearly stated that laminar flow becomes the theoretical best, once control energy is accounted for, and that driving a successful flow-control strategy towards either maximized savings or maximized performance is something left to the specific application. Awareness of the importance of energy considerations, related to spanwise forcing, is steadily increasing [41].

In its early days, spanwise forcing was not particularly attractive in terms of global energy savings. The spanwise-oscillating wall (SOW), i.e. the simplest form of spanwise forcing, consists of an alternating movement of the wall in the spanwise direction, as

$$v(x, y, 0, t) = A \sin(\omega t)$$

where v is the spanwise component of the velocity at the wall, i.e. at $z = 0$, A is the maximum velocity along the cycle, and ω is the oscillating frequency. Known has been since long time [11] that in a turbulent wall-bounded flow the sudden application of a spanwise pressure gradient causes a drop in the streamwise friction, and that a sinusoidally varying spanwise pressure gradient (or, equivalently, a sinusoidal spanwise movement of the wall) makes this effect sustained in time. However, the impressive values of skin-friction reduction reported in the early SOW studies (up to 40-50%, see [27]) were not balanced against the energy cost of the actuation. Baron & Quadrio [4] were first to measure the energy expenditure of SOW, and found that – in an idealized scenario where actuation has unitary efficiency – a tiny amount of net savings is achievable, provided that the forcing amplitude remains moderate. Although the practical appeal of SOW remained scarce, this result was in principle extremely interesting, insofar as it attested the possibility to interact with the complex turbulence dynamics using a simplistic control, and to achieve an overall positive gain, thus motivating the continuation of the research effort. The SOW technique was later comprehensively assessed by Quadrio and Ricco in [51].

More than one decade later, and still leading the way of the international efforts, the present authors established [56] that a purely spatial oscillation is equivalent (in fact, slightly superior) to the temporal one, thus opening the way to exploitation of the spanwise-forcing concept with passive mechanisms. The following forcing type was studied:

$$v(x, y, 0, t) = A \sin(kx)$$

where the temporal oscillation at frequency ω is replaced by a spatial oscillation along the streamwise direction with wavelength $2\pi/k$.

The breakthrough came in 2009, with the discovery by Quadrio, Ricco and Viotti [53] that a combined spatio-temporal oscillation brings superior drag reduction properties and a vastly improved energy balance. They introduced the following forcing:

$$v(x, y, 0, t) = A \sin(kx - \omega t) \tag{6}$$

and found that the combined forcing, which takes the form of a streamwise-traveling wave of spanwise wall velocity, exhibits several interesting properties, most prominently a relatively small energy required for the forcing, and leads

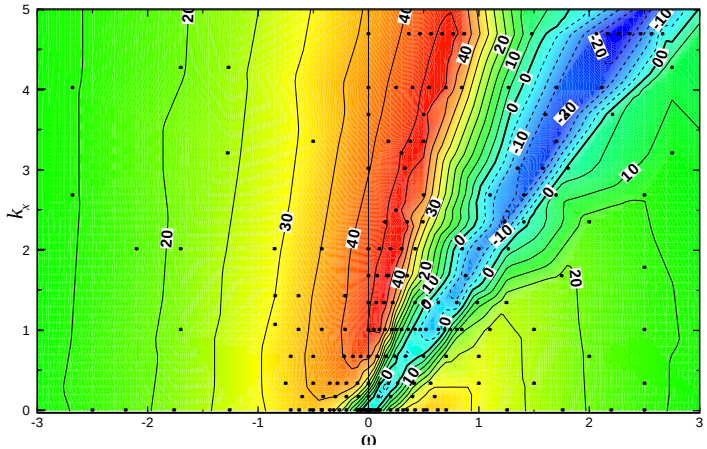

Fig. 4. Map of the drag reduction(red)/increase(blue) as a function of wavenumber and frequency of the forcing, for $A^+ = 12$ in a turbulent channel flow at $\mathrm{Re}_\tau = 200$. Figure taken from [53].

to a maximum *net* drag reduction of more than 20%. A map of measured drag reduction as a function of wavenumber and frequency is plotted in Fig. 4. Drag reduction was found to be well predicted by properties of the spanwise boundary layer created by the forcing, named the "Generalized Stokes Layer" [52] as it contains as a special case the classic Stokes layer that develops when an indefinite wall oscillates beneath a still fluid.

Only one year after writing [53], the same group at Politecnico di Milano demonstrated the streamwise-travelling-wave concept experimentally, with a test that so far has yielded one of the largest measured drag reductions ever (neary 40%), and probably the largest net saving. The experiment was designed in a pipe flow configuration, and the wall forcing was realized through an alternate azimuthal movement of thin ring-like slices of the pipe, independently actuated via a shaft-and-belt system (see fig.5). Use of water as the working fluid, and the relatively low value of Re, allowed design and implementation of a mechanical actuator that cannot scale up to realistic applications, but was definitely effective in a proof-of-principle experiment.

The combination of large benefits and relative ease of implementation make the spanwise forcing in the form of streamwise-travelling waves one of the best candidates for applications. The most relevant issue that remains still open is the lack of a suitable actuator with the required high efficiency, low cost, low weight, and high control authority (large velocities, actuation frequencies, etc): good candidates indeed exist, but none is ready for industrial applications. Several other concerns, though, have been successfully addressed in the meantime. An important one was that, until recently, all the available information on spanwise forcing, collected via DNS or experiments, was related to low-Re flows. Extrapolating available information to application-level Re indicated a rapid decrease

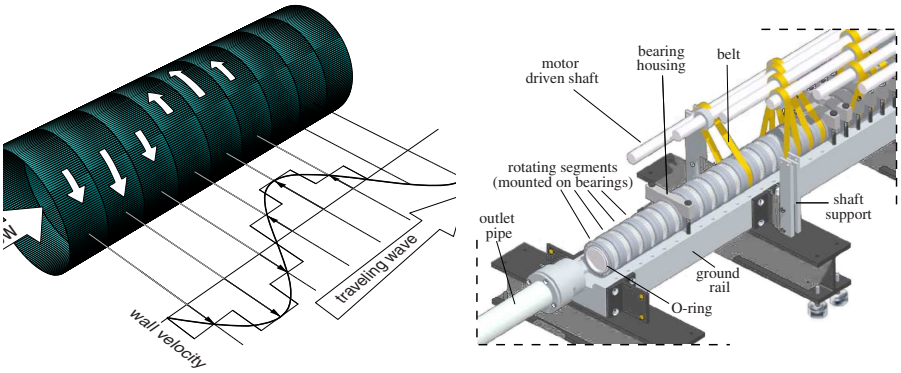

Fig. 5. Conceptualization of the actuation strategy to implement forcing (6), and sketch of the experimental setup for the drag-reduction experiment of the PoliMI pipe. Figures taken from [2].

of the performance of drag reduction. This was until a large-scale campaign of numerical experiments carried out by Gatti and Quadrio [22] demonstrated that spanwise forcing is equivalent to a drag-decreasing roughness, discussed above in § 4, and shares with it its Reynolds-number dependence embodied in (5), which was extended to account for larger values of ΔB. They carried out more than 4,000 DNS at two well-separated values of Re, and made it possible to extrapolate drag reduction at any Re: according to their data, the reduction of turbulent friction attainable on an airplane in cruise flight via spanwise forcing remains remarkable, in the order of 30%.

Finally, it is emerging that to reduce the skin friction (by spanwise forcing, or by other means) has the potential to bring in additional benefits when the application involves a body with complex shape (an airplane, for example) where turbulent friction is only one of the sources for aerodynamic drag. The original suggestion originated once again in Italy, thanks to RANS simulations of riblets on an airplane carried out by Mele and Tognaccini [43], and was later investigated with DNS. Banchetti *et al.* [3] applied spanwise forcing to the incompressible flow over a bump, and found benefits for pressure drag too; ongoing work is demonstrating the same concept on a wing section in transonic flight, where spanwise forcing is successful in altering the position of the shock wave.

6 Concluding remarks

In this chapter four aspects of turbulent flow in proximity of a wall have been reviewed, all four being the subject of very active and ongoing research: the shape

of the mean velocity profile and the applicability limits and precise values of the coefficients of the classical logarithmic law, the statistics of turbulent fluctuations and their multi-dimensional characterization in space-time, the passive (static) surface modifications that may offer some reduction in skin-friction drag, and the active (moving-wall) modifications that may offer a larger reduction at the expense of greater complication. These are just examples of the open research problems that the mystery of turbulence exposes, and we hope that the progress made up to now may be an incentive for the Italian Mechanics community to keep on devoting energies towards their solution.

References

1. Afzal, N.: Millikan's argument at moderately large Reynolds number. Phys. Fluids **19**(4), 600–602 (1976)
2. Auteri, F., Baron, A., Belan, M., Campanardi, G., Quadrio, M.: Experimental assessment of drag reduction by traveling waves in a turbulent pipe flow. Phys. Fluids **22**(11), 115103/14 (2010)
3. Banchetti, J., Luchini, P., Quadrio, M.: Turbulent drag reduction over curved walls. J. Fluid Mech. **896** (2020)
4. Baron, A., Quadrio, M.: Turbulent drag reduction by spanwise wall oscillations. Appl. Sci. Res. **55**, 311–326 (1996)
5. Baron, A., Quadrio, M., Vigevano, L.: On the boundary layer/riblets interaction mechanism and the prediction of the turbulent drag reduction. Int. J. Heat Fluid Flow **14**(4), 324–332 (1993)
6. Bechert, D., Bartenwerfer, M.: The viscous flow on surfaces with longitudinal ribs. J. Fluid Mech. **206**, 105–209 (1989)
7. Bechert, D., Bruse, M., Hage, W., van der Hoeven, J., Hoppe, G.: Experiments on drag-reducing surfaces and their optimization with an adjustable geometry. J. Fluid Mech. **338**, 59–87 (1997)
8. Benzi, R., De Angelis, E., L'vov, V.S., Procaccia, I., Tiberkevich, V.: Maximum drag reduction asymptotes and the cross-over to the Newtonian plug. J. Fluid Mech. **551**, 185–195 (2006)
9. Bernardini, M., Pirozzoli, S., Orlandi, P.: Velocity statistics in turbulent channel flow up to Re_τ=4000. J. Fluid Mech. **742**, 171–191 (2014)
10. Bernardini, M., Modesti, D., Salvadore, F., Pirozzoli, S.: STREAmS: A high-fidelity accelerated solver for direct numerical simulation of compressible turbulent flows. Computer Physics Communications **263**, 107906 (2021)
11. Bradshaw, P., Pontikos, N.: Measurements in the turbulent boundary layer on an 'infinite' swept wing. J. Fluid Mech. **159**, 105–130 (1985)
12. Chiarini, A., Mauriello, M., Gatti, D., Quadrio, M.: Ascending-descending and direct-inverse cascades of Reynolds stresses in turbulent Couette flow. J. Fluid Mech., in press. arXiv:2109.03522v1 [physics.flu-dyn] (2021)
13. Cimarelli, A., De Angelis, E., Casciola, C.: Paths of energy in turbulent channel flows. J. Fluid Mech. **715**, 436–451 (2013)
14. Cimarelli, A., De Angelis, E., Jimenez, J., Casciola, C.: Cascades and wall-normal fluxes in turbulent channel flows. J. Fluid Mech. **796**, 417–436 (2016)
15. Cimarelli, A., De Angelis, E., Schlatter, P., Brethouwer, G., Talamelli, A., Casciola, C.: Sources and fluxes of scale energy in the overlap layer of wall turbulence. J. Fluid Mech. **771**, 407–423 (2015)

16. De Angelis, E., Casciola, C.M., L'vov, V.S., Piva, R., Procaccia, I.: Drag reduction by polymers in turbulent channel flows: Energy redistribution between invariant empirical modes. Phys. Rev. E **67**(5), 056312 (2003)
17. De Angelis, E., Casciola, C.M., L'vov, V.S., Pomyalov, A., Procaccia, I., Tiberkevich, V.: Drag reduction by a linear viscosity profile. Phys. Rev. E **70**(5), 055301 (2004)
18. Frohnapfel, B., Hasegawa, Y., Quadrio, M.: Money versus time: Evaluation of flow control in terms of energy consumption and convenience. J. Fluid Mech. **700**, 406–418 (2012)
19. Furuichi, N., Terao, Y., Wada, Y., Tsuji, Y.: Friction factor and mean velocity profile for pipe flow at high Reynolds numbers. Phys. Fluids **27**(9), 095108 (2015)
20. Gatti, D., Chiarini, A., Cimarelli, A., Quadrio, M.: Structure function tensor equations in inhomogeneous turbulence. J. Fluid Mech. **898**, A5–33 (2020)
21. Gatti, D., Quadrio, M.: Performance losses of drag-reducing spanwise forcing at moderate values of the Reynolds number. Phys. Fluids **25**, 125109(17) (2013)
22. Gatti, D., Quadrio, M.: Reynolds-number dependence of turbulent skin-friction drag reduction induced by spanwise forcing. J. Fluid Mech. **802**, 553–58 (2016)
23. Hasegawa, Y., Quadrio, M., Frohnapfel, B.: Numerical simulation of turbulent duct flows at constant power input. J. Fluid Mech. **750**, 191–209 (2014)
24. Hill, R.: Equations relating structure functions of all orders. J. Fluid Mech. **434**, 379–388 (2001)
25. Jiménez, J., Moser, R.D.: What are we learning from simulating wall turbulence? Philos. Trans. R. Soc. Math. Phys. Eng. Sci. **365**(1852), 715–732 (2007)
26. Johnstone, R., Coleman, G.N., Spalart, P.R.: The resilience of the logarithmic law to pressure gradients: Evidence from direct numerical simulation. J. Fluid Mech. **643**, 163–175 (2010)
27. Jung, W., Mangiavacchi, N., Akhavan, R.: Suppression of turbulence in wall-bounded flows by high-frequency spanwise oscillations. Phys. Fluids A **4 (8)**, 1605–1607 (1992)
28. Kim, J., Moin, P., Moser, R.: Turbulence statistics in fully developed channel flow at low Reynolds number. J. Fluid Mech. **177**, 133–166 (1987)
29. Luchini, P.: Effects of riblets on the growth of laminar and turbulent boundary layers. In: Choi, K.-S. et al. (ed.) 7th European Drag Reduction Meeting Berlin 1992, pp. 101–116, Mechanical Engineering Publications, UK (1996)
30. Luchini, P.: Reducing the turbulent skin friction. In: Desideri et al. (ed.) Computational Methods in Applied Sciences 1996. pp. 465–470, Wiley (1996)
31. Luchini, P.: Linearized no-slip boundary conditions at a rough surface. J. Fluid Mech. **737**, 349–367 (2013)
32. Luchini, P.: Structure and interpolation of the turbulent velocity profile in parallel flow. Eur. J. Mech. B/Fluids **71**, 15–34 (2018)
33. Luchini, P., Manzo, F., Pozzi, A.: Resistance of a grooved surface to parallel flow and cross-flow. J. Fluid Mech. **228**, 87–109 (1991)
34. Luchini, P., Quadrio, M.: A low-cost parallel implementation of direct numerical simulation of wall turbulence. J. Comp. Phys. **211**(2), 551–571 (2006)
35. Luchini, P., Quadrio, M., Zuccher, S.: Phase-locked linear response of a turbulent channel flow. Phys. Fluids **18**(121702), 1–4 (2006)
36. Luchini, P.: Universality of the turbulent velocity profile. Phys. Rev. Lett. **118**(22), 224501 (2017)
37. Luchini, P.: An elementary example of contrasting laminar and turbulent flow physics. arXiv:1811.11877 [physics.flu-dyn] (2018)

38. Luchini, P.: Law of the wall and law of the wake in turbulent parallel flow. In: Örlü, R. et al. (eds.) Progress in Turbulence VIII. pp. 63–68. Springer Proceedings in Physics, Springer International Publishing, Cham (2019)
39. Mansour, N., Kim, J., Moin, P.: Reynolds-stress and dissipation-rate budgets in a turbulent channel flow. J. Fluid Mech. **194**, 15–44 (1988)
40. Marusic, I., McKeon, B.J., Monkewitz, P.A., Nagib, H.M., Smits, A.J., Sreenivasan, K.R.: Wall-bounded turbulent flows at high Reynolds numbers: Recent advances and key issues. Phys. Fluids **22**(6), 065103 (2010)
41. Marusic, I., Chandran, D., Rouhi, A., Fu, M.K., Wine, D., Holloway, B., Chung, D., Smits, A.J.: An energy-efficient pathway to turbulent drag reduction. Nat Commun **12**(1), 5805 (2021)
42. Marusic, I., Monty, J.P., Hultmark, M., Smits, A.J.: On the logarithmic region in wall turbulence. J. Fluid Mech. **716** (2013)
43. Mele, B., Tognaccini, R.: Slip length–based boundary condition for modeling drag reduction devices. AIAA J. **56**(9), 3478–3490 (2018)
44. Monkewitz, P.A.: The late start of the mean velocity overlap log law at – a generic feature of turbulent wall layers in ducts. J. Fluid Mech. **910** (2021)
45. Oliver, T., Malaya, N., Ulerich, R., Moser, R.: Estimating uncertainties in statistics computed from direct numerical simulation. Phys. Fluids **26**, 035101 (2014)
46. Pirozzoli, S., Romero, J., Fatica, M., Verzicco, R., Orlandi, P.: One-point statistics for turbulent pipe flow up to $\mathrm{Re}_\tau \approx 6000$. J. Fluid Mech. **926** (2021)
47. Quadrio, M.: Drag reduction in turbulent boundary layers by in-plane wall motion. Phil. Trans. R. Soc. A **369**(1940), 1428–1442 (2011)
48. Quadrio, M., Luchini, P.: Direct numerical simulation of the turbulent flow in a pipe with annular cross-section. Eur. J. Mech. B/Fluids **21**, 413–427 (2002)
49. Quadrio, M., Luchini, P.: The linear response of a turbulent channel flow. In: Advances in Turbulence IX: Proceedings of the Ninth European Turbulence Conference, pp. 715–718, CIMNE, UK (2002)
50. Quadrio, M., Luchini, P.: Integral space–time scales in turbulent wall flows. Phys. Fluids **15**(8), 2219–2227 (2003)
51. Quadrio, M., Ricco, P.: Critical assessment of turbulent drag reduction through spanwise wall oscillation. J. Fluid Mech. **521**, 251–271 (2004)
52. Quadrio, M., Ricco, P.: The laminar generalized Stokes layer and turbulent drag reduction. J. Fluid Mech. **667**, 135–157 (2011)
53. Quadrio, M., Ricco, P., Viotti, C.: Streamwise-traveling waves of spanwise wall velocity for turbulent drag reduction. J. Fluid Mech. **627**, 161–178 (2009)
54. Russo, S., Luchini, P.: The linear response of turbulent flow to a volume force: Comparison between eddy-viscosity model and DNS. J. Fluid Mech. **790**, 104–127 (2016)
55. Russo, S., Luchini, P.: A fast algorithm for the estimation of statistical error in DNS (or experimental) time averages. J. Comp. Phys. **347**, 328–340 (2017)
56. Viotti, C., Quadrio, M., Luchini, P.: Streamwise oscillation of spanwise velocity at the wall of a channel for turbulent drag reduction. Phys. Fluids **21**, 115109 (2009)
57. Virk, P.S.: Drag reduction fundamentals. AIChE J. **21**(4), 625–656 (1975)
58. Zhu, X., Phillips, E., Spandan, V., Donners, J., Ruetsch, G., Romero, J., Ostilla-Mónico, R., Yang, Y., Lohse, D., Verzicco, R., Fatica, M., Stevens, R.J.A.M.: AFiD–GPU: A versatile Navier–Stokes solver for wall-bounded turbulent flows on GPU clusters. Computer Physics Communications **229**, 199–210 (Aug 2018)